

Electronic Structure

Structure of Nanocrystals in Hexagonal SiC after Ge, Si and Er Implantation

U. Kaiser[1], A. Chuvilin[2], D. Muller[3], W. J. Choyke[4]

[1]Friedrich-Schiller-Universität Jena, Germany; [2]Institute of Catalysis, Russia;
[3]Bell Laboratories, USA; [4]University of Pittsburgh, USA

Hole and Electron Effective Masses in 6H-SiC Studied by Optically Detected Cyclotron Resonance

N. T. Son[1], C. Hallin[2], E. Janzén[1]

[1]Linköping University, Sweden; [2]ABB Corporate Research, Sweden

Photoreflectance Characterization of GaNAs/GaAs Multiple Quantum Well Structures

C. R. Lu[1], Y. Y. Chen[1], J. R. Lee[1], W. I. Lee[2], S. C. Lee[2]

[1]National Taiwan Normal University, ROC; [2]National Chiao Tung University, ROC

Photoluminescence and Electroluminescence Characterisation of InGaN/GaN Multiple Quantum Well Light Emitting Diodes

P. J. Bergman[1], G. Pozina[1], B. Monemar[1], M. Iwaya[2], S. Nitta[2], H. Amano[2],
I. Akasaki[2]

[1]Linköping University, Sweden; [2]Meijo University, Japan

Towards Quantum Structures in SiC (Invited)

F. Bechstedt

Friedrich-Schiller-Universität Jena, Germany

STRUCTURE OF NANOCRYSTALS IN HEXAGONAL SiC AFTER Ge, Si AND ER IMPLANTATION

U. Kaiser, A. Chuvilin, D. A. Muller, W. J. Choyke

¹*Friedrich-Schiller-Universität Jena, Institut für Festkörperphysik, Max-Wien-Platz 1,
D-07743 Jena, Germany
Tel.: +49-3641-947445, Fax.: +49-3641-947442, e-mail: kaiser@pinet.uni-jena.de
Institute of Catalysis, Lavrentjeva 5, Novosibirsk 90630090, Russia
Bell Laboratories 700 Mountain Avenue, Murray Hill, NJ 079749
Dept. of Physics and Astronomy University of Pittsburgh Pittsburgh, PA, USA. 15260*

Properties of bulk materials can be modified significantly if the material is manipulated at the nanometre scale. In particular, the growth of Si and Ge nanostructures constitutes a promising approach for the development of light emitting devices [1]. Hexagonal SiC is a promising matrix candidate because of its wide band gap. Techniques such as ion-implantation can be used to fabricate nanostructures in SiC [2, 3], in which effective interband transitions can be expected for Ge dots [4]. However only strained nanocrystals of defined uniform size (below 5nm) show significant quantum effects. Therefore basic structure determination of the nanocrystals is required.

The structure of nanocrystals in 4H and 6H SiC after Si 100keV, Ge 250keV and Er 400keV ion implantation and a fluence of ($1 \times 10^{17} \text{cm}^{-2}$) at high temperature (700°C) followed by annealing at 1500°C and 1600°C has been investigated by advanced microscopy carried out in JEOL 3010, 2010F TEMs using high-resolution (HR) imaging, energy dispersive X-ray (EDX) spectroscopy, electron energy-loss spectroscopy (EELS) and high-angle annular dark field scanning electron microscopy (ADF-STEM) imaging. Digitally acquired HR images were analyzed to determine lattice fringe spacings within nanocrystals using the Diffpack plug-in from Digital Micrograph [5].

For the case of Ge and Er implantation, the nanocrystals have been revealed and their size distribution has been determined from Z-contrast images showing that the medium size is about 5nm with a distribution width from 2 to 10 nm. As results from lattice fringe spacing analysis of HRTEM images, main part of the Er-containing nanocrystals are unstrained ErSi₂ (P6/mmm) oriented with their c-axis parallel to the c-axis of the SiC matrix. For the case of Si implantation, hexagonal Si nanocrystals have been revealed with their c-axis parallel or inclined to the c-axis of

the matrix. The lattice fringe spacing analysis revealed nanocrystal strain of about 4 %. For the case of Ge implantation, GeSi crystals have been formed. Applying the strain value for the Si nanocrystals as a first approximation to the GeSi crystals, from the lattice fringe spacing analysis the Ge content could be determined and compared to results from EDX point analysis, EELS core level shift, and the ADF contrast (see the figure). Molecular dynamic (MD) simulations followed by high-resolution image simulations are carried out to investigate the strain state of the nanodots. Most nanocrystals revealed are strained hexagonal GeSi, with their c-axis parallel, inclined or perpendicular to the c-axis of the SiC matrix. For selected cases, the unoccupied densities of states for the GeSi nanocrystals have been obtained from EELS. Photoluminescence measurements on Er and Ge implanted specimens are carried out in addition.

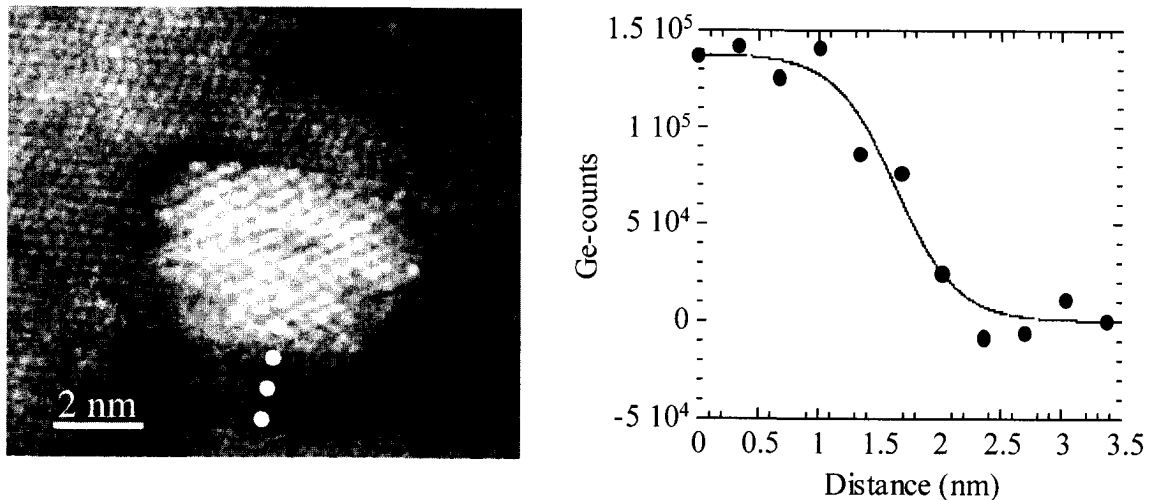


Figure Atomic resolution ADF-STEM image of a GeSi nanocrystal on the left and the Ge content along the dotted line obtained from EELS measurements.

The financial support of the Deutsche Forschungsgemeinschaft (SFB 196) is gratefully acknowledged.

References

- [1] Pavébi L, DalNegro L, Mozzoleni C, Franco G, Priolo F, Nature 408 (2000) 440
- [2] U. Kaiser, A. Chuvilin, W. Richter, G. Pasold, W. Witthuhn, Chr. Schubert, W. Wesch, W. J. Choyke, Conference Proceedings, Widegap2001, Exeter March 2001, GB
- [3] U. Kaiser, J. Electron Microscopy, 50 (2001)
- [4] F. Bechstedt (2001) private communication
- [5] User manual Digital Micrograph, Gatan, Inc. Pleasanton, C. A.

Hole and electron effective masses in 6H-SiC studied by optically detected cyclotron resonance

N.T. Son¹, C. Hallin², and E. Janzén¹

¹Department of Physics and Measurement Technology, Linköping University, S-581 83 Linköping, Sweden

Tel: 46-13-282531, Fax: 46-13-142337, e-mail: son@ifm.liu.se

²ABB Corporate Research, S-721 78 Västerås, Sweden

The effective masses of electrons and holes in semiconductors are fundamental parameters, which are required for many analyses. The most direct method for determination of effective masses is cyclotron resonance (CR). The observation of a well-defined CR requires $\omega\tau > 1$, with ω being the cyclotron frequency used in the experiments and τ the carrier scattering time. In SiC crystals available nowadays, the carrier mobility is rather low due to short carrier scattering time caused by high density of defects and residual impurities. It is therefore very difficult to satisfy the requirement of $\omega\tau > 1$ for conventional CR experiments in SiC. Using optically detected cyclotron resonance (ODCR) with its advantages of improving the mobility due to photoneutralization of ionised impurities, we have previously been able to determine the effective masses of electrons and holes in 4H-SiC [1,2] and of electrons in 6H-SiC [3] at X-band (~9.23 GHz) and Q-band (~35 GHz) frequencies. However, in our previous studies [3], the electron effective masses in 6H-SiC were determined with a large uncertainty due to a very broad ODCR line width caused by short carrier scattering time. The hole mobility is often lower than that of electrons. This makes it difficult to satisfy the CR condition for holes, and therefore, the hole effective masses in 6H-SiC have not been experimentally studied so far.

In this work, we report our ODCR determination of the hole effective masses and more accurate effective mass values for electrons in 6H-SiC. Using high purity free-standing 6H-SiC layers grown by chemical vapour deposition with low concentration of residual impurities (N donor: $\sim 4 \times 10^{14} \text{ cm}^{-3}$, Al and B acceptors are below 10^{14} cm^{-3}), we have observed two well-separated ODCR peaks, which are labelled e-CR and h-CR and illustrated in figures 1(a) and 1(b). Complete angular dependencies of both ODCR peaks were obtained and analyzed. The angular dependence of the h-CR peak can be described by the usual cyclotron mass relation for the case of an elliptical energy surface, with the best fit values of the transverse mass $m_{\perp}(h) = (0.67 \pm 0.01) m_0$ and the longitudinal mass $m_{\parallel}(h) = (1.85 \pm 0.03) m_0$. The principal axis of the ellipsoid is parallel to the direction of the c-axis. Considering all possible alternatives, this ODCR signal can only be attributed to the CR of the hole. These values are similar to the hole effective masses in 4H-SiC [$m_{\perp}(h) = 0.66 m_0$ and $m_{\parallel}(h) = 1.75 m_0$] [2] and are close to the calculated values by Persson et al [4] with taking into account the polaron effect [$m_{\perp}(h) = 0.65 m_0$ and $m_{\parallel}(h) = 1.80 m_0$]. At low microwave power (~3.1 mW), no noticeable changes in the position or the line shape of the h-CR peak could be detected when rotating the magnetic field in the (0001) plane. This indicates that the hole effective mass is isotropic in the basal plane and the valence band close to its maximum is parabolic.

The e-CR peak is related to the CR of electrons. For the first time, a complete angular dependence of the e-CR has been obtained. When the magnetic field approaches the direction perpendicular to the c-axis, the peak moves to high magnetic fields and becomes very broad [the line width at half maximum is about 145 mT as can be seen in Fig. 1(b)]. Because of the

line broadening, it was not possible to resolve the anisotropy of the electron effective masses in the basal plane as predicted by theory [4]. The analysis of the angular dependence is therefore based on the model of an elliptical energy surface with the transversal mass, $m_{\perp}(e)$, being the average of the mass components in the basal plane and the longitudinal mass, $m_{\parallel}(e)$, is the mass along the direction of the c-axis. The obtained electron effective masses are $m_{\perp}(e)=(0.48\pm 0.01) m_0$ and $m_{\parallel}(e)=(5.65\pm 0.15) m_0$. This $m_{\perp}(e)$ value is slightly larger than the value previously determined [$m_{\perp}(e)=0.42 m_0$] in Ref. 3. The value determined in our previous work [3] is not so accurate (due to a small $\omega\tau$ value of only ~ 1.2 , the OCDR peak is not well defined). The $m_{\parallel}(e)$ value of $5.65 m_0$ in this case is much larger than the value $m_{\parallel}(e)=(2.0\pm 0.2) m_0$ that we obtained before [3]. It is likely that in our previous work [3], the broad CR peak, which obtained at the magnetic field directions close to the direction perpendicular to the c-axis, was the CR of holes but not electrons (in this direction of the magnetic field, the CR of electrons may be not observable due to too short scattering time).

The influence of the polaron effect on the electron and hole effective masses in 6H-SiC will be discussed.

References

- [1] D. Volm et al, Phys. Rev. B **53**, 15409 (1996).
- [2] N.T. Son et al, Phys. Rev. B **61**, R10544 (2000).
- [3] N.T. Son et al, Appl. Phys. Lett. **65**, 3209 (1994).
- [4] C. Persson et al, J. Appl. Phys. **82**, 5496 (1997).

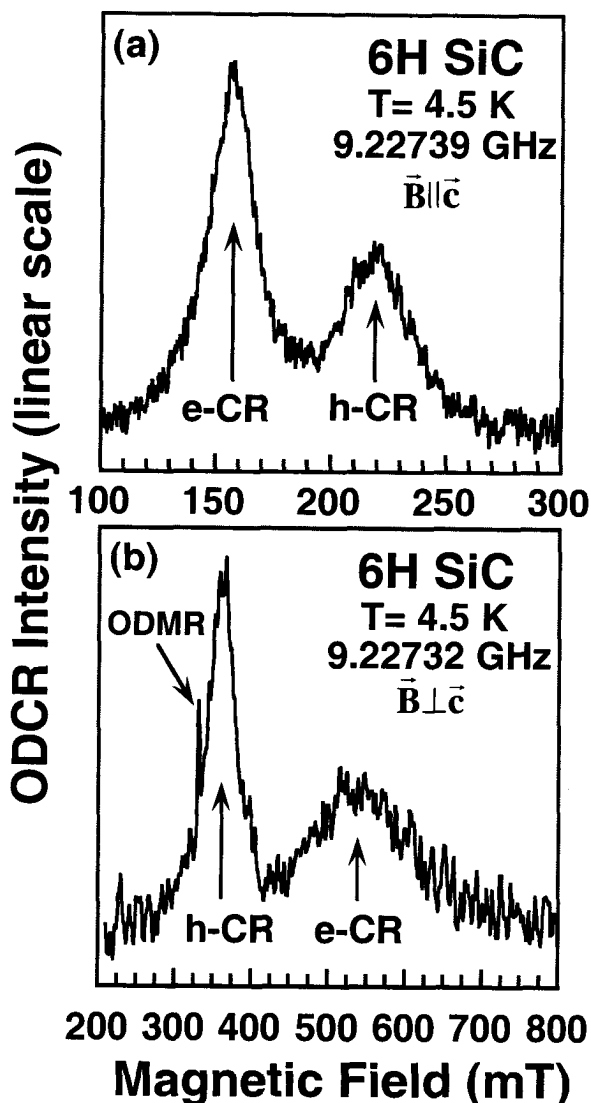


Fig. 1. ODCR spectra observed in 6H-SiC with monitoring the near band-edge luminescence for the magnetic field \mathbf{B} (a) parallel and (b) perpendicular to the c-axis ($\mathbf{B} \parallel [11\bar{2}0]$). The peaks corresponding to the cyclotron resonance of the electrons and holes are labelled e-CR and h-CR, respectively. The microwave power is (a) 0.1 mW and (b) 3.1 mW. The sample was excited by the 334.5 nm line of an Ar ion laser with a power of 5 mW and the beam was defocused to a large spot on the sample. The sharp peak near 330.5 mT is related to an optically detected magnetic resonance (ODMR) signal of a defect.

Photoreflectance Characterization of GaNAs/GaAs Multiple Quantum Well Structures

Chien-Rong Lu¹, Yo-Yu Chen¹, Jia-Ren Lee¹, Wei-I Lee², Shih-Chang Lee²

¹Department of Physics, National Taiwan Normal University, Taipei, Taiwan, 116, ROC

E-mail address: lupond@phy03.phy.ntnu.edu.tw

Tel: 886-2-29346620 Ext.133

Fax: 886-2-29326408

²Department of Electrophysics, National Chiao Tung University, Hsinchu, Taiwan 300, ROC

Nitrogen containing III-V alloys like GaNAs have drawn considerable attention recently because of their interesting physical properties and a wide range of possible optoelectronic applications. However fundamental properties such as the bowing parameter, effective masses, the band alignment and the electronic states in the heterostructure systems are not well understood. There are still discrepancies among different experimental results and different theoretical predictions. Further experimental studies are needed. We report the photoreflectance (PR) spectroscopy studies of the GaNAs/GaAs multiple-quantum-well (MQW) structures at various temperatures.

The investigated structures were grown by the MOCVD. The MQW structures consist of 20 periods of GaN_xAs_{1-x}/GaAs layers. The GaAs layers were all 25 nm thick. The nitrogen compositions of the GaN_xAs_{1-x} layers in different MQW structures were varied up to x=0.04, and their thickness were 10nm or 6nm. A tungsten-halogen lamp with a monochromator provides the probing photons for the PR spectroscopy. The 514 nm line of an Ar⁺ ion laser through a light chopper provides the pumping photons to generate electron hole pairs for the internal field modulation. Using the phase lock-in technique, the electro-modulated optical responses of the excitonic transition are enhanced, and the band edge transition exhibits Franz-Keldysh oscillatory (FKO) features whose period indicates the strength of the internal field. These spectral characters make the PR experiment one of the best spectroscopic probe for the electrooptical properties.

The PR spectra from different GaNAs/GaAs (MQW) structures at 75K are compared in the Fig. 1. Although the band gap energy of GaN is larger than that of GaAs, the GaN_xAs_{1-x} alloy show a considerable red shift of the band edge with increasing nitrogen concentration for low x-values. Instead of being barriers, the GaN_xAs_{1-x} alloys become wells in the GaNAs/GaAs (MQW) structures under investigation, and the excitonic interband transitions of the MQW systems were observed in the spectral range above $h\nu = E_g(\text{GaN}_x\text{As}_{1-x})$ as indicated in the Fig.1. Comparing spectrum (a) and spectrum (b) from MQW structures with the same nitrogen composition (x=0.04) but of different well width, the MQW transition

features are blue shifted while the well width reduced from 10 nm to 6 nm as shown in Fig.1. The blue shift is also observed when nitrogen composition is reduced from $x=0.04$ to $x=0.017$ as shown by spectrum (a) and spectrum (c) in Fig.1. A matrix transfer algorithm was used to match the $\text{GaN}_x\text{As}_{1-x}/\text{GaAs}$ boundary conditions and calculate the MQW subband energies numerically. The bowing parameter, effective masses, and the band-offset values were adjusted to obtain the $\text{GaN}_x\text{As}_{1-x}/\text{GaAs}$ MQW subband energies to best fit the observed optical transition features. These fundamental parameters are important for further studies of the optoelectronic properties of the GaNAs heterostructure quantum systems.

The oscillatory features labeled FKO(GaAs) and FKO(GaNAs) are the FKO cause by the pumping photons induced modulation of the internal electric field in the GaAs region and that in the $\text{GaN}_x\text{As}_{1-x}$ region respectively. The extrema in the FKO features of an electro-modulated spectrum are given by

$$n\pi = \phi + \frac{3}{4} \left[\frac{(E_n - E_g)}{\hbar\Theta} \right]^{3/2}, \quad (1)$$

Where n is the index number of the n th extrema, ϕ is an arbitrary phase factor, E_n is the photon energy of the n th oscillation extrema, and E_g is the band gap energy. The electrooptical energy $\hbar\Theta$ is defined by $(\hbar\Theta)^3 = e\hbar^2 F^2 / (2\mu)$, where F is the internal electric field, and μ is the reduced interband effective mass. A plot of $(E_n - E_g)^{3/2}$ versus n yields a straight line with a slope proportional to the internal electric field. The composition and the temperature variations of the internal electric field are analyzed.

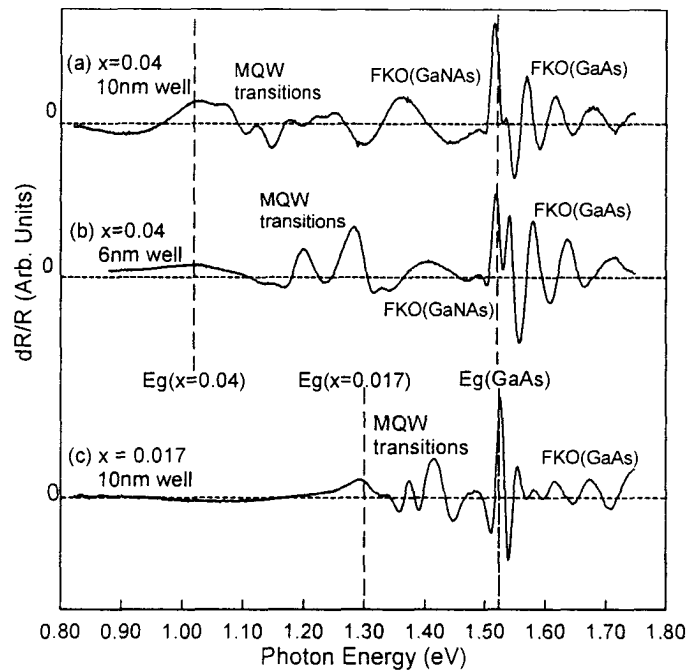


Fig1. Comparison of the PR spectra of GaNAs/GaAs MQW with different well widths and N compositions x .

PHOTOLUMINESCENCE AND ELECTROLUMINESCENCE CHARACTERIZATION OF InGaN/GaN MULTIPLE QUANTUM WELL LIGHT EMITTING DIODES STRUCTURES

J. P. Bergman, G. Pozina, and B. Monemar

*Department of Physics and Measurement Technology, Linköping University,
S-581 83 Linköping, Sweden*

Tel: +46 13 282382. Fax: +46 13 142337. Email: ped@ifm.liu.se

M. Iwaya, S. Nitta, H. Amano, and I. Akasaki

*Department of Electrical Engineering and Electronics and High-Tech Research Center, Meijo
University, 1-501 Shiogamaguchi, Tempaku-ku, Nagoya 468-8502, Japan*

InGaN/GaN multiple quantum well (MQW) structures are currently of significant interest due to their application for the active region in blue-violet light emitting diodes and lasers. We report on optical studies, photoluminescence and electroluminescence, of heterostructures consisting of four InGaN quantum wells (QWs) (content of In is 11 %) grown on top of a GaN layer with micrometer-sized mass-transport areas [1]. Ti/Au and Ti/Al were used as contacts for anode and cathode, respectively. PL emissions are measured through the semitransparent top contact. The diode structure shows good structural and optical properties.

The combination of electroluminescence with photoluminescence using pulsed excitation provides an efficient method to separately measure the contribution from the optical and the electrical injection, by synchronized time integration of the emission with the pulsed laser excitation. Using the pulsed optical excitation we have also studied the time decay of the different emissions.

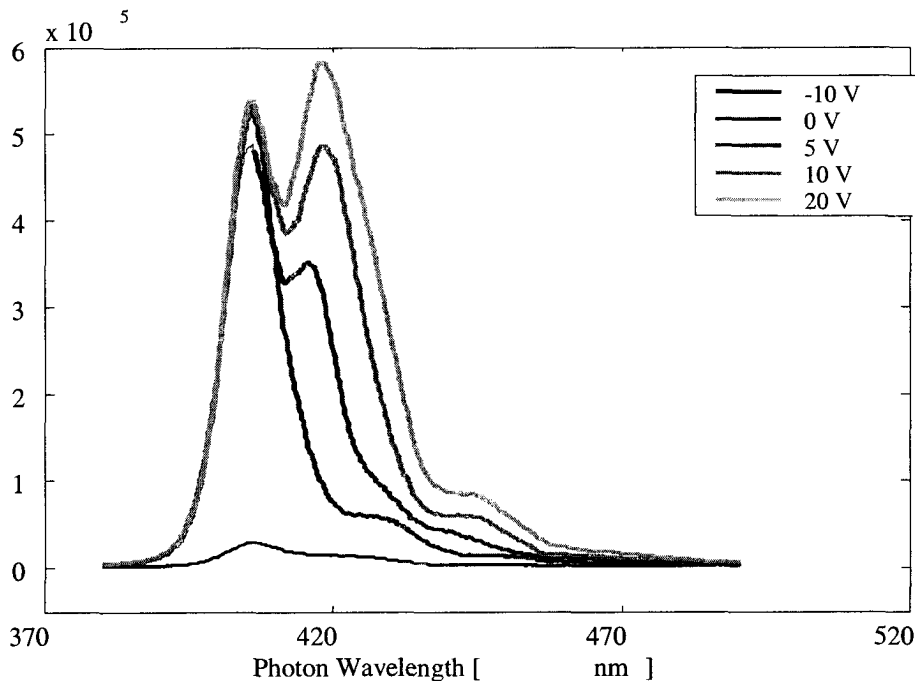


Fig 1 Time integrated PL spectra (0-20 ns) with different bias voltage.

The photoluminescence (PL) spectrum demonstrates several peaks at low temperature. The PL is dominated by the rather narrow near-bandgap emission at 3.07 eV with a linewidth of 40 meV.

This emission has a typical PL decay time about few ns at 2 K within the PL contour. However, we have observed an additional well-resolved line with the lower peak energy. Its position depends strongly on excitation conditions and is about 3.00 meV under a cw excitation with the laser beam power of 50 mW. The PL decay time for this second emission is longer than for the 3.07 eV line at least by one order of magnitude. To explain the origin of these two strong lines we suggested a model in which at least two nonequivalent quantum wells could be realized due to a potential gradient across the layers [1]. To verify this model we have applied an external electrical field to vary the internal potential across the heterostructure. Spectral positions, relative PL intensities as well as the PL transients and decay times have been measured as a function of electrical field and temperature for the different PL peaks. The PL data are comparable with electroluminescence spectra from the same diode. Our experimental data set, we believe, are helpful in understanding of the recombination mechanism in the InGaN/GaN MQW structures.

[1]. G. Pozina, J. P. Bergman, B. Monemar, M. Iwaya, S. Nitta, H. Amano and I. Akasaki, *Appl. Phys. Lett.* 77, 1638 (2000).

Towards quantum structures in SiC

Friedhelm Bechstedt*

Friedrich-Schiller-Universität, Institut für Festkörpertheorie und Theoretische Optik, Max-Wien-Platz 1, 07743 Jena, Germany
Tel.: +49-3641-947150, Fax: +49-3641-947152, E-mail: bechstedt@ifto.physik.uni-jena.de

The use of the quantum confinement effect to tailor the electronic, optical, and electrical properties is accompanied by an enormous progress in the field of semiconductor physics and devices. The fabrication of low-dimensional structures with electron confinement in one, two, or three dimensions is based on heterostructures of two different semiconductors. The different energetical positions of their conduction (valence) bands give rise to an energy barrier for the electrons (holes). Prototypical structures are semiconductor superlattices and quantum dot arrays.

From the point of view of quantum-confined structures, SiC is an extremely promising material. More than 200 polytypes with different stacking of the atomic Si-C bilayers in [0001] direction exist. The fundamental energy gap varies by about 1 eV between the cubic zinc-blende (3C) polytype and hexagonal (nH) polytypes with a number of n Si-C bilayers in a unit cell. Consequently, the growth of heteropolytypic structures makes it possible to build devices from heterostructures consisting of one specific semiconducting material but occurring in different crystal structures [1,2]. Indeed, there is a remarkable progress in the growth of heteropolytypic structures using solid-source molecular beam epitaxy (MBE) [3]. Another class of quantum structures are Si and also Ge dots. Embedding the group-IV dots in a wide-band-gap semiconductor, as hexagonal SiC, electroinjection of electron-hole pairs should be possible. Very recently the self-organized growth of Si and Ge dot arrays on a SiC surface has been demonstrated [4,5].

In this talk ideas, realizations, and properties of quantum structures based on SiC will be discussed. Two prototypical systems are studied. First, the attention is focussed onto SiC heterostructures. The MBE growth of the cubic polytype occurs preferentially under more Si-rich conditions, i.e. at lower temperatures (e.g. $T = 1550$ K). The hexagonal polytypes, however, were grown under less Si-rich conditions corresponding to slightly higher temperatures (e.g. 1600 K). As an example, a resulting 4H/3C/4H double heteropolytypic structure is presented in Fig. 1.



Fig. 1: TEM micrograph of a 4H/3C/4H-SiC(0001) double-heteropolytypic structure [3].

Meanwhile, the growth of multiple heterostructures consisting of some dozens of 4H-SiC barriers and of 3C-SiC wells was performed by solid-source MBE on 3° off-axis 4H substrates. The photoluminescence spectra measured for these multiple heterocrystalline structures show signals below the band gap of the 3C polytype, hence, indicating the type-II character of the heterostructure. A corresponding band structure calculated for a 3C/4H-SiC superlattice is presented in Fig. 2. The pronounced subband structure below the conduction

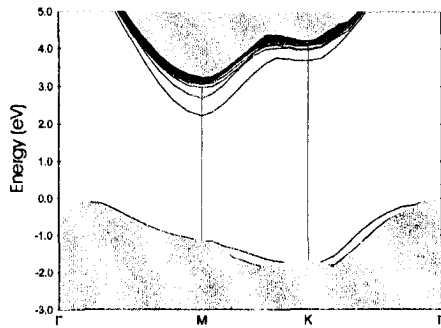


Fig. 2 Band structure of a $(3C)_3(4H)_{15}$ -SiC(0001) superlattice. The shaded regions indicate the projected bulk band structure of 4H-SiC. Quasiparticle effects are taken into account.

band minimum of 4H-SiC indicates deep quantum wells for the electrons in the 3C regions. The band structure is still indirect in k -space parallel to the interfaces, so that the observed luminescence lines may be a consequence of the break of the k -selection rule by phonons and imperfections of the grown structure. An extremely large built-in electric field in the 3C layers allows a tunneling of the hole wave functions into the 3C regions resulting in a spatial overlap with the electron functions and, hence, optical transitions within the 3C regions.

Second, other interesting quantum structures are Si or Ge nanocrystallites embedded in SiC that can be fabricated by MBE or ion implantation with subsequent annealing. From a theoretical point of view we suggest the preparation in particular of Ge dots in hexagonal SiC. Calculations [6] have shown that, even for Ge nanocrystallites with a diameter of about 2 nm, there are optical transitions at the absorption edge which possess oscillator strength comparable with those of III-V compounds. This tendency can be also seen from the absorption spectrum of Ge dots embedded in 3C-SiC in Fig. 3. A low-energy peak occurs which shows a redshift and an increasing strength with rising dot size. Whereas the k -selection rule is broken in the Ge case, the indirect character of Si occurs already for not too

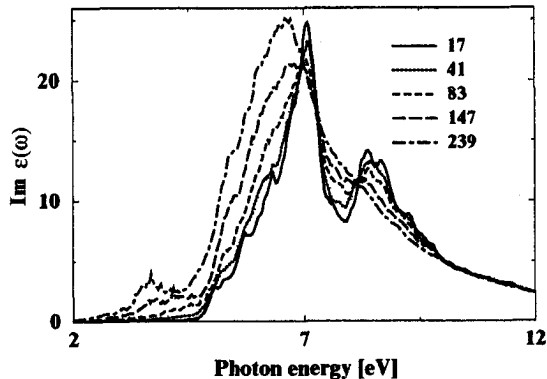


Fig. 3 Imaginary part of the dielectric function of Ge dots with varying number of atoms embedded in 3C-SiC. Results are obtained using a 512-atom supercell.

large nanocrystallites. The hexagonal SiC polytypes should be used as matrix material. Only in this case a type-I heterostructure situation with a localization of electrons and holes in the Ge nanocrystallites is predicted.

* *in collaboration with A. Fissel, J. Furthmüller, K. Goetz, U. Grossner, U. Kaiser, K. Komlev, J. Kräußlich, W. Richter B. Schröter, C. Schubert, A. Stekolnikov, H.-C. Weissker, and W. Wesch*

- [1] M. Ruf, H. Hitlehner, and R. Helbig, *IEEE Electronic Devices* **41**, 1040 (1994).
- [2] F. Bechstedt and P. Käckell, *Phys. Rev. Lett.* **75**, 264 (1995).
- [3] A. Fissel, B. Schröter, U. Kaiser, and W. Richter, *Appl. Phys. Lett.* **77**, 2418 (2000).
- [4] A. Fissel, K. Pfennighaus, and W. Richter, *Thin Solid Films* **318**, 88 (1998).
- [5] B. Schröter, K. Komlev, U. Kaiser, G. Heß, G. Kipshidze, and W. Richter, *Materials Science Forum* **353-356**, 247 (2001).
- [6] H.-C. Weissker, J. Furthmüller, and F. Bechstedt, *Phys. Rev. B* (submitted).